

EARTH RESONANT GRAVITY ASSISTS FOR ASTEROID RETRIEVAL MISSIONS

Joan Pau Sánchez CuartiellesDepartment of Applied Mathematics I, Universitat Politècnica de Catalunya, Barcelona, Spain
jpau.sanchez@upc.edu**Elisa Maria Alessi**IFAC-CNR, Sesto Fiorentino (FI), Italy
em.alessi@ifac.cnr.it**Daniel García Yáñez**Department of Mechanical and Aerospace Engineering, University of Strathclyde, Glasgow, UK.
Daniel.garcia-yarnoz@strath.ac.uk**Colin McInnes**Department of Mechanical and Aerospace Engineering, University of Strathclyde, Glasgow, UK.
colin.mcinnnes@strath.ac.uk

Asteroids and comets are of strategic importance for science in an effort to uncover the formation, evolution and composition of the Solar System. Near-Earth objects (NEOs) are of particular interest because of their accessibility from Earth, but also because of their speculated wealth of material resources. The possibility of retrieving entire NEOs from accessible heliocentric orbits and moving them into the Earth's neighbourhood is today a credible possibility considered by NASA, within its Asteroid Initiative Framework, and examined in several recent scientific publications. This paper searches for asteroid retrieval trajectories that benefit from several resonant Earth encounters to decrease at each encounter the transfer Δv cost. Particularly, the paper focuses on the Amor asteroid population, which have the encounters always occurring outside the Earth's sphere of influence. Thus, the patched conic approximation is rendered essentially not applicable. Numerical exploration in the framework of the Circular Restricted Three Body Problem (CR3BP) becomes computationally expensive when combined with the sensitivities of multiple Earth encounters. Hence, this paper proposes a 3D extension of the energy kick function to rapidly assess all possible third-body effects into the asteroid's trajectory. The osculating elements of the asteroid can be updated by means of Picard's first iteration on each Keplerian element, where the perturbing forces of the third body (i.e., the Earth) are given by the Lagrange's planetary equations. This allows a rapid scanning process of sequences of Earth encounters that may in turn allow a favourable perturbation to the asteroid orbital elements.

I. INTRODUCTION

In recent years, significant interest has been devoted to the understanding of minor bodies of the Solar System, including near-Earth and main belt asteroids and comets. NASA, ESA and JAXA have conceived a series of missions to obtain data from such bodies, having in mind that their characterisation not only provides a deeper insight into the formation of the Solar System, but also represents a technological challenge for space exploration. Near Earth Objects (NEOs) in particular have also stepped into prominence because of two important issues: they are among the easiest bodies to reach from the Earth and they may represent a potential impact threat.

The debate on the potential for future exploitation of NEOs, and possible synergies with science [1] and planetary protection, is clearly intensifying in recent years. Evidence can be found in the growing body of scientific literature on the topic of asteroid

exploitation, as well as in recent mission proposals, such as the Keck asteroid retrieval mission [2], and in the interest from the commercial space sector in their potential resources*.

Indeed, the interest for these neighbouring celestial bodies may have reached a tipping point early this year with two important events: the Chelyabinsk meteor, which was intensively covered by media, and the announcement of NASA's latest mission concept within the Asteroid Initiative Framework: to rendezvous with an asteroid, lasso it and haul it back to Earth neighbourhood to then being visited by astronauts by 2021†.

Inspired by all of this, a recent publication [3] puts forward a new subcategory of asteroids: the Easily Retrievable Objects, or EROs. These are Near Earth Objects that can be gravitationally captured in bound

* <http://www.planetaryresources.com/>

† http://www.nasa.gov/sites/default/files/files/AsteroidRedirectMission_FS_508_2.pdf

periodic orbits around the collinear libration points L_1 and L_2 of the Sun-Earth system under a certain Δv threshold, which was arbitrarily selected in García et al. [3] as 500 m/s.

García et al. [3] describe a robust methodology to search among a vast number of near Earth asteroids for advantageous candidates for retrieval missions. The retrieval trajectories considered aimed at the insertion of the asteroid into a periodic libration points orbits. These libration point orbits (LPOs) can also serve as target gateways to other Sun-Earth-Moon system orbits of interest, through transit orbits inside Earth's Hill sphere and heteroclinic connections between libration points.

García et al. [3] however considered only retrieval trajectories that target the Earth at the following Earth encounter. The work thus disregarded the possibility of taking advantage of multiple Earth encounters in order to obtain further benefit from third-body effects that may decrease the transfer costs even more. Clearly, the reason not to consider multiple Earth encounters was that this type of transfers entails very long times of flight, since the synodic period for retrieval targets tends to be very large. This paper however will not consider transfer time constraints and will thus explore the possibility of long Earth resonant sequences.

Dynamical system theory provides effective methodologies to compute quasi-ballistic transfers, however exploring a full set of these trajectories can become computationally expensive, and even more so when combined with the sensitivities of multiple Earth encounters. Hence, this paper also proposes an alternative method for preliminary design of low-energy transfers exploiting multiple Earth resonant gravity assists.

Instead of the computationally expensive process of numerically propagating a large set of stable invariant manifold trajectories, we propose to use a 3D extension of the energy kick function [4] to rapidly assess all possible third-body effects into the asteroid's trajectory. The osculating elements of the asteroid can be updated by means of Picard's first iteration on each Keplerian element, where the perturbing forces of the third body (i.e., the Earth) are given by the Lagrange's planetary equations. This allows a rapid scanning process of sequences of Earth encounters that may in turn allow a favourable perturbation to the asteroid orbital elements. The procedure can then be used to optimise sequences of gravity assists for realistic target objects for asteroid retrieval missions.

II. EASILY RETRIEVABLE OBJECTS

Current interplanetary spacecraft have masses on the order of 10^3 kg, while an asteroid of 10 meters diameter will most likely have a mass of the order of

10^6 kg. Hence, already moving such a small object, or an even larger one, with the same ease that a scientific payload is transported today, would demand propulsion systems orders of magnitudes more powerful and efficient; or alternatively, orbital transfers orders of magnitude less demanding than those to reach other planets in the Solar System.

Solar System transport phenomena, such as the rapid orbital transitions experienced by comets Oterma and Gehrels 3, from heliocentric orbits with periaapsis outside Jupiter's orbit to apoapsis within Jupiter's orbit, or the Kirkwood gaps in the main asteroid belt, are some manifestations of the sensitivities of multi-body dynamics. The same underlying principles that enable these phenomena allow also excellent opportunities to design surprisingly low energy transfers.

II.1 Low Energy Transport conduits

As is well known, the phase space near the equilibrium regions in the CR3BP can be divided into four broad classes of motion; bound motion near the equilibrium position, asymptotic trajectories that approach or depart from the latter, transit trajectories, and, non-transit trajectories (see Figure 1).

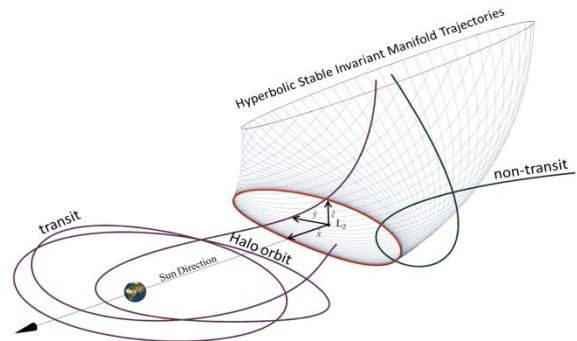


Figure 1: Schematic representation of the four categories of motion near the L_2 point (represented by the set of axes in the figure): periodic motion around L_2 (i.e., halo orbit), hyperbolic invariant manifold structure (i.e., set of stable hyperbolic invariant manifold trajectories), transit trajectory and non transit trajectory.

In García et al. [3], a systematic search for asteroids whose unperturbed trajectories laid close to stable invariant manifold trajectories belonging either to planar Lyapunov, vertical Lyapunov or Halo orbits was performed. A final list with 12 objects was provided whose trajectories fulfilled the requirement that they could be modified with impulsive manoeuvres below a total cost of 500 m/s and set into a stable manifold trajectory leading to a bound motion near the Earth. This final list of asteroids is reproduced here in Table 1.

	a	e	i	MOID	Diameter	Δv
	[AU]		[deg]	[AU]	[m]	[m/s]
2006 RH120	1.033	0.024	0.595	0.0171	2.3- 7.4	2Hn 0.058
						2Hs 0.107
						2V 0.187
						2P 0.298
2010 VQ98	1.023	0.027	1.476	0.0048	4.3-13.6	2V 0.181
						2Hs 0.393
						2Hn 0.487
						2P 0.199
2007 UN12	1.054	0.060	0.235	0.0011	3.4-10.6	2Hn 0.271
						2Hs 0.327
						2V 0.434
						2Hn 0.249
2010 UE51	1.055	0.060	0.624	0.0084	4.1-12.9	2P 0.340
						2V 0.470
						2Hs 0.474
						2P 0.328
2008 EA9	1.059	0.080	0.424	0.0014	5.6-16.9	1Hn 0.356
						1V 0.421
						1Hs 0.436
						2Hs 0.392
2009 BD	1.062	0.052	1.267	0.0053	4.2-13.4	2V 0.487
						2Hs 0.393
2008 UA202	1.033	0.069	0.264	$2.5 \cdot 10^{-4}$	2.4- 7.7	2P 0.425
						2Hn 0.467
						2V 0.400
2011 BL45	1.033	0.069	3.049	0.0040	6.9-22.0	2V 0.400
2011 MD	1.056	0.037	2.446	0.0018	4.6-14.4	2V 0.422
2000 SG344	0.978	0.067	0.111	$8.3 \cdot 10^{-4}$	20.7-65.5	1P 0.443
						1Hs 0.449
						1Hn 0.468
1991 VG	1.027	0.049	1.445	0.0037	3.9-12.5	2Hn 0.465
						2V 0.466

Table 1: ERO characteristics for transfer trajectories with Δv below 500 m/s. The type of transfer is indicated by a 1 or 2 indicating L_1 or L_2 plus the letter P for planar Lyapunov, V for vertical Lyapunov, and Hn or Hs for north and south halo.

II.II Targeting capture trajectories

A hyperbolic invariant manifold structure, such as the one depicted in Figure 1, consists of an infinite set of trajectories associated with bound motion near the equilibrium position. Particularly, the stable set consists of an infinite number of trajectories exponentially approaching a periodic or quasi-periodic orbit. Thus, if an asteroid's unperturbed orbit lies near one of these trajectories, a gentle push may insert the object into a trajectory leading to a bound motion near the Earth.

When the set of trajectories forming the stable invariant manifold are close to the Earth, they need to be propagated numerically using the equations of motion of the CR3BP. However, if the distance to Earth is large, these orbits behave as any other classical Keplerian orbit.

Hence, in [3], these stable invariant trajectories were propagated backwards to a planar section located at a $\pi/8$ angle with the Sun-Earth line. This section corresponds roughly to a distance to Earth of

the order of 0.4 AU, where the gravitational influence of the planet can already be considered small. From this section outwards, these trajectories could then be well approximated in two-body motion, and thus described analytically by means of their constant orbital elements. These constant orbital elements at the $\pi/8$ section are independent of the final insertion time under the CR3BP assumption. Note that the only exception is the longitude of the perihelion, i.e., the sum of the right ascension of the ascending node and the argument of perihelion, which varies with a simple function of time due to the motion of the Earth on its orbit [2].

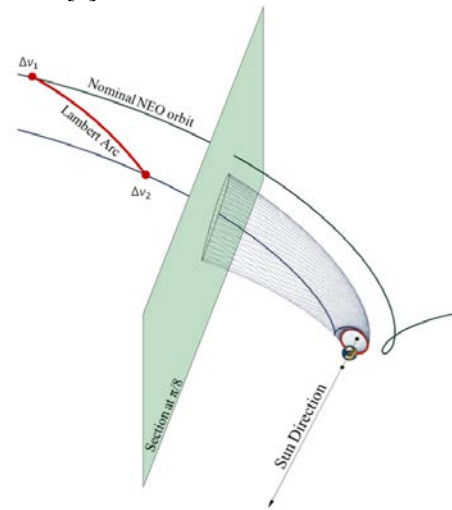


Figure 2: Schematic representation of a transfer to L_2

Finally, as depicted in Figure 2, the sets of orbital elements associated with stable invariant manifold trajectories at the $\pi/8$ section can be used as a *bullseye* orbit targeting for Earth capture trajectories. The targeting can be solved by means of a heliocentric Lambert arc of a restricted two-body problem with two impulsive burns, one to depart from the NEO, the final one for insertion into the manifold, with the insertion constrained to take place before the arrival at the section.

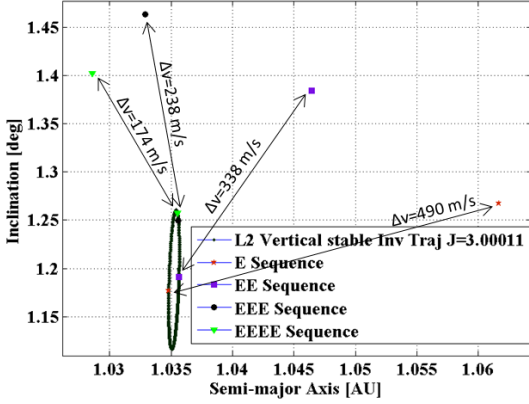


Figure 3: Capture opportunities of asteroid 2009 BD during consecutive encounters of the Earth, if these encounters were trimmed to achieve beneficial third body effects.

Figure 3 shows an example of a capture transfer as found in [3]. It was found that asteroid 2009 BD could be captured in a vertical Lyapunov orbit with Jacobi constant of 3.00011 by means of a Δv manoeuvre costing 490 m/s. As proposed by this paper, by trimming the right encounter with the Earth, which will be discussed further in later sections, it will be shown here that during an hypothetical second encounter with the Earth the same asteroid could be captured into the same periodic orbit with a Δv of 338 m/s. If allowed further revolutions in the synodic reference frame, a third encounter capture could be achieved with 238 m/s, and finally during a fourth encounter with 174 m/s.

II.III Pruning: The Analytic Transfer.

The search for asteroid retrieval opportunities carried out in [3] required to explore a vast catalogue of NEOs (~9,000 objects). Hence, preliminary pruning of objects that did not offer a good chance for low cost capture opportunities became a necessity, due to the high computational costs involved in optimizing a retrieval trajectory.

With this purpose, a filter based on a Δv cost estimate computed as a bi-impulsive transfer with both burns assumed at aphelion and perihelion was implemented. Either of the two burns is also responsible for correcting the inclination required to reach a given invariant manifold trajectory. The Δv required to modify the semi-major axis can be expressed as:

$$\Delta v_a = \sqrt{\mu_s \left(\frac{2}{r} - \frac{1}{a_f} \right)} - \sqrt{\mu_s \left(\frac{2}{r} - \frac{1}{a_0} \right)} \quad (1)$$

where μ_s is the Sun's gravitational constant, a_0 and a_f are the initial and final semi-major axis before and after the burn, and r is the distance to the Sun at which the burn is made (perihelion or aphelion

distance). On the other hand the Δv required to modify the inclination at either apsis can be approximated by:

$$\Delta v_i = 2 \sqrt{\frac{\mu_s}{a_0} r^* \sin(\Delta i / 2)} \quad (2)$$

where Δi is the required inclination change, and r^* corresponds to the ratio of perihelion and aphelion distance if the burn is performed at aphelion, or its inverse if performed at perihelion.

The total estimated cost is then calculated as:

$$\Delta v_t = \sqrt{\Delta v_{a1}^2 + \Delta v_{i1}^2} + \sqrt{\Delta v_{a2}^2 + \Delta v_{i2}^2} \quad (3)$$

with one burn performed at each of the apsis, and one of the two inclination change Δv assumed zero. The estimated transfer Δv corresponds thus to the minimum of four cases: aphelion burn modifying perihelion and inclination followed by a perihelion burn modifying aphelion, perihelion burn modifying aphelion and inclination followed by an aphelion burn modifying perihelion, and the equivalent ones in which the inclination change is done in the second burn.

Note that Eq.(1) and Eq.(2) only take into consideration the shape and inclination of the orbits, ignoring the rest of the orbital elements: the right ascension of the ascending node Ω and argument of pericentre ω . Hence, the resultant estimates from Eq. (3) would correspond to the theoretical minimum for a Lambert arc transfer, if phasing was optimal. Nevertheless, as will be shown later, the results of the filter provide a rather accurate estimate of the transfer and will be used in this paper to assess the resonant encounter sequences that provide a better chance to reduce the costs of an asteroid retrieval trajectory.

III. EARTH RESONANT ENCOUNTERS

In a similar fashion to the multiple Earth and Venus gravity assist, introduced by Hollenbeck [5], that is today commonly used to decrease the cost to reach the outer planets, the following sections aim to investigate the feasibility to introduce one or multiple Earth encounters on the asteroid capture trajectories investigated in [3] in order to achieve further reduction of the transfer Δv at the cost of larger transfer times.

This paper however focuses its efforts on a subcategory of near Earth asteroid that does not cross the orbit of the Earth, i.e., the Amor objects. This places a further constraint on the analysis of the 'endgame problem' [6] (as the search for energy-reducing series of flybys before the final capture into a planetary body is generally referred to). That is due to the fact that Amor orbits will never encounter the Earth within its sphere of influence, and thus, the

patched conic approximation is rendered essentially not applicable.

It is therefore necessary either to perform a numerical exploration in the CR3BP, or alternatively use a general perturbation method capable to describe the third-body effects when relatively close to the secondary. Hence, the classical Legendre polynomial expansion of the third-body disturbing function [7] cannot be applied here since it requires the distance to the test particle (e.g., spacecraft or asteroid) to be much smaller than the distance to the perturbing body.

The use of a 3D extension of the energy kick function previously developed by other authors [4] for a planar case is thus here investigated. The intention is to build an approximated perturbing force that by means of Picard's first iteration allows us to update each orbital element after an Earth encounter. Hence, if a semi-analytical tool to estimate the motion in the CR3BP is available, a global search for favourable encounter sequences can be made effectively.

IV. KEPLERIAN MAP

Considering the restricted case of the 3BP, the Hamiltonian in the inertial reference frame of a test particle moving within a 3D CR3BP framework can be written as:

$$H_{iner} = \frac{1}{2}(p_x^2 + p_y^2 + p_z^2) - \frac{1-\mu}{r_1} - \frac{\mu}{r_2} \quad (4)$$

where p_x , p_y and p_z are the conjugate momenta, μ the non-dimensional mass parameter and r_1 and r_2 the distance to the primary and secondary mass of the system, respectively (i.e., Sun and Earth in the case at hand, as shown in Figure 4).

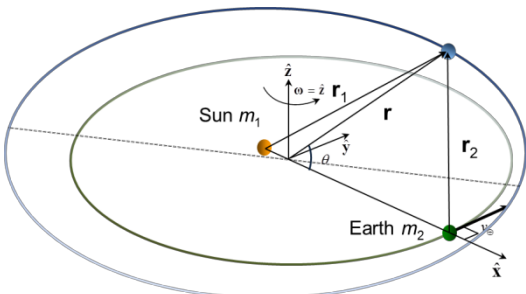


Figure 4: Relationship between distances in the three-body problem.

The distances to the primary r_1 and secondary r_2 can be described with spherical coordinates (r, θ) , where r is the distance from the barycentre to the test particle and θ the angle between \hat{r} and the direction between the primaries \hat{x} . Thus, by the law of cosines, r_1 and r_2 can be expressed as:

$$r_1^2 = r^2 + \mu^2 - 2r\mu \cos(\pi - \theta) \quad (5)$$

$$r_2^2 = r^2 + (1-\mu)^2 - 2r(1-\mu) \cos \theta$$

The mass parameter μ considered in this paper is $3.0032080443 \times 10^{-6}$ (note that this neglects the mass of the Moon). In Eq. (4) μ is a small parameter, and thus suitable to be used to describe the perturbation of the secondary mass on the 2 body motion of an object orbiting the primary mass.

Since $\mu/r \ll 1$, the r_1 distance can be written as:

$$r_1 = r + \mu \cos \theta + O(\mu^2) \quad (6)$$

using Taylor series and truncating to the first order in μ . Hence Eq. (4) can be rewritten as:

$$H_{iner} = \left(\frac{1}{2}(p_x^2 + p_y^2 + p_z^2) - \frac{1}{r} \right) + \mu \left(\frac{1}{r} + \frac{\cos \theta}{r^2} - \frac{1}{r_2} \right) + O(\mu^2) \quad (7)$$

Finally, μ/r_2 can also be truncated to the first order in μ , which allows us to write more conveniently:

$$H_{iner} = K + \mu R + O(\mu^2) \quad (8)$$

where K is the 2-body problem Hamiltonian and R the first order perturbed part, expressed as:

$$R = -\frac{1}{\sqrt{1+r^2-2r\cos\theta}} + \frac{\cos\theta}{r^2} + \frac{1}{r} \quad (9)$$

The angle θ between \hat{r} and \hat{x} direction can be described as a function of the osculating elements of the test particle as:

$$\cos \theta = \cos \Omega_{rot} \cdot \cos(\nu + \omega) - \sin \Omega_{rot} \cdot \sin(\nu + \omega) \cdot \cos i \quad (10)$$

where Ω_{rot} is the ascending node of the test particle measured from the rotating \hat{x} direction, thus $\Omega - \nu_{\oplus}$,

where ν_{\oplus} is the true anomaly of the secondary object.

Finally, since R is a small perturbation and we can still assume that the main motion of the test particle is going to be a Keplerian orbit, r can then be expressed as:

$$r = \frac{p}{1 + e \cos \nu} \quad (11)$$

The above description allows us to express Eq. (9) as a function of Keplerian elements, and it is thus well suited to be integrated by means of Lagrange's Planetary Equations in order to obtain a good estimate of the rate of change of the osculating elements.

IV.I Semi-major axis kick

Expressing the first order perturbed potential as:

$$R' = \mu R, \quad (12)$$

the variation of semi-major axis can be written as:

$$\frac{da}{dt} = \mu \frac{2b}{nr^2} \frac{\partial R}{\partial \nu} \quad (13)$$

Integrating Eq.(13) over an entire orbit, the rate of semi-major axis change per orbit is obtained:

$$\Delta a = \mu \frac{2b}{n} \int_{-T/2}^{T/2} \frac{1}{r^2} \frac{\partial R}{\partial v} dt \quad (14)$$

Note that, similarly to Ross and Scheeres [4], the integration is performed from the periaapsis passage. The complete orbit is then integrated by integrating half an orbit backwards and half forward. This was considered convenient, among other reasons to minimize possible problems during the numerical integration procedure, but a priori other integration limits may be possible.

Equation (14) can be more conveniently integrated as a function of true anomaly:

$$\Delta a = \mu \frac{2}{an^2} \int_{-\pi}^{\pi} \frac{\partial R(a, e, i, \Omega_{rot}(\Omega, t(v)), \omega, v)}{\partial v} dv. \quad (15)$$

Note that in Eq.(15) Ω_{rot} is a function of time, which is expressed as a function of true anomaly, thus the integration does not resolve trivially. The full integration is summarized in the Appendix, which is currently solved by means of MATLAB's *quadl* function, a high order method using an adaptive Gauss/Lobatto quadrature rule.

IV.II Inclination kick

The rate of change of the inclination during an Earth encounter can be computed as:

$$\frac{di}{dt} = \mu \left(\frac{\cos i}{nab \sin i} \frac{\partial R}{\partial \omega} - \frac{1}{nab \sin i} \frac{\partial R}{\partial \Omega} \right), \quad (16)$$

which, as in the case of the semi-major axis, can be more conveniently computed as:

$$\Delta i = \frac{\mu}{n^2 a^2 b^2 \sin i} \left(\cos i \int_{-\pi}^{\pi} r^2 \frac{\partial R}{\partial \omega} dv - \int_{-\pi}^{\pi} r^2 \frac{\partial R}{\partial \Omega} dv \right) \quad (17)$$

Complete integration is presented also in the Appendix section, and as in the previous case, is currently solved by means of MATLAB's *quadl* function.

IV.III Eccentricity kick

The rate of change in eccentricity can be readily estimated using the Tisserand parameter as a first order approximation of the Jacobi Constant of the moving particle, which should remain constant along the entire trajectory. Hence,

$$\Delta e = e_f - e_0 \quad (18)$$

where e_f can be estimated as:

$$e_f = \sqrt{1 - \frac{1}{a_0 + \Delta a} \left(\frac{T_0 - \frac{1}{a_0 + \Delta a}}{2 \cos(i_0 + \Delta i)} \right)^2} \quad (19)$$

and T_0 is the constant Tisserand parameter:

$$T_0 = \frac{1}{a_0} + 2\sqrt{a_0(1-e_0^2)} \cos(i_0) \quad (20)$$

IV.IV Argument of periaapsis kick

The rate of change of the argument of the periaapsis can also be estimated as:

$$\frac{d\omega}{dt} = \frac{b}{na^3 e} \frac{\partial R}{\partial e} - \frac{\cos i}{nab \sin i} \frac{\partial R}{\partial i}, \quad (21)$$

which resolves into an integral such as:

$$\Delta \omega = \frac{1}{n^2 a^4 e} \int_{-\pi}^{+\pi} r^2 \frac{\partial R}{\partial e} dv - \frac{\cos i}{(nab)^2 \sin i} \int_{-\pi}^{+\pi} r^2 \frac{\partial R}{\partial i} dv \quad (22)$$

IV.V Integrated results and accuracy

In order to assess how well Eq. (15), (17), (18) and (22) reproduce the orbital evolution of a particle moving within the framework of the CR3BP, we can now compare the orbital changes resultant of the above integrations with a propagation in the CR3BP. This is done for series of different sets of (a, e, i, ω) taken from interesting accessible asteroids found during previous work [3].

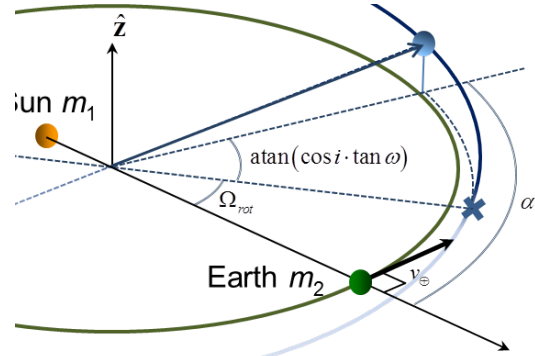


Figure 5: Description of the angle α of the encounter.

The actual encounter undergone by a (a, e, i, ω) set is uniquely defined by the angular distance between the Sun-Earth line and the projection of the periaapsis line in the Earth orbital plane at the moment of the periaapsis passage, here referred as α as described in Figure 5. Hence, by scanning all possible α angles for a set of (a, e, i, ω) we obtain an overall picture of the consequences of an Earth encounter for different encounter geometries (i.e., phasings). By comparing the results of these encounters propagated with CR3BP and the integrations described in this section we also obtain an estimate of its accuracy for different cases. This is done in the following manner: a set of $(a, e, i, \omega, \alpha)$ defines the conditions at the periaapsis with a given angular distance with the Earth. This set is both integrated using the Keplerian map and propagated half an orbit backwards and half an orbit forward in the CR3BP. The results are plotted for one case in Figure 6 to Figure 9.

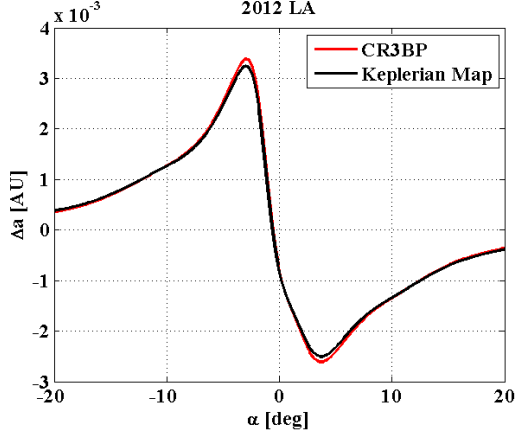


Figure 6: Semi-major axis kick as a function of the angular distance of the periapsis passage for a 2012 LA-like orbit (1.04 AU, 0.023, 3.13 deg).

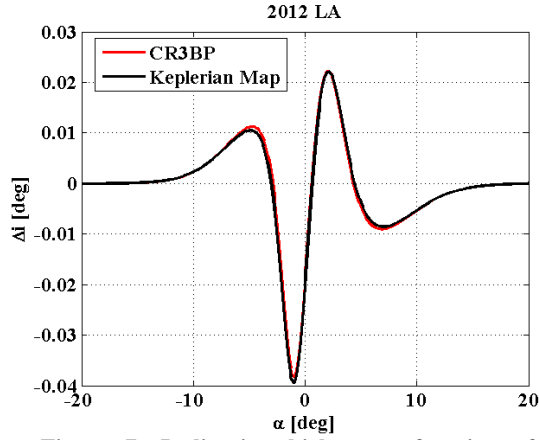


Figure 7: Inclination kick as a function of the angular distance of the periapsis passage for a 2012 LA-like orbit (1.04 AU, 0.023, 3.13 deg).

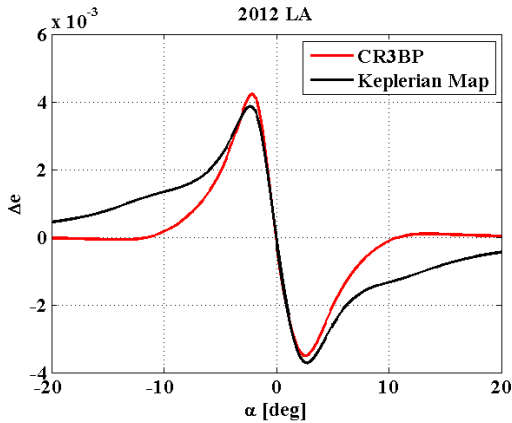


Figure 8: Eccentricity kick as a function of the angular distance of the periapsis passage for a 2012 LA-like orbit (1.04 AU, 0.023, 3.13 deg).

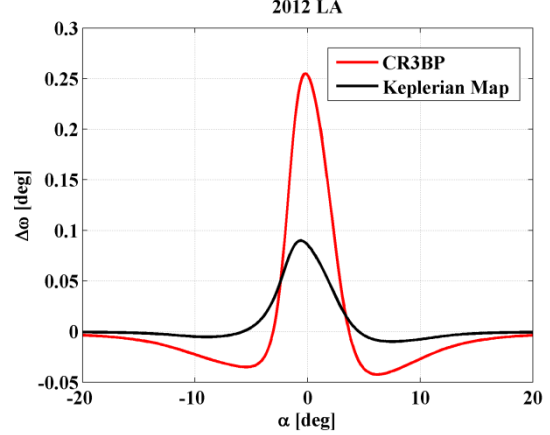


Figure 9: Argument of the periapsis ω kick as a function of the angular distance of the periapsis passage for a 2012 LA-like orbit (1.04 AU, 0.023, 3.13 deg).

A simple visual inspection of Figure 6 to Figure 9 already suggests a high accuracy for the integrated results compared with the CR3BP prediction, especially for semi-major axis and inclination. This accuracy however needs to be set into context, before deciding about the quality of the integrated results. Firstly, the results from equations (15) to (22) are intended for a rapid assessment of the consequences of an encounter with the Earth. The type of encounter that asteroid 2012 LA undergoes with the Earth, for example, could not be reproduced by other classical approximations of astrodynamics, such as the patched conic approximation, and would require at a minimum a CR3BP framework to be understood. The integrals above provide a reasonable approximation without the need to propagate numerically the motion, which is a very useful advantage when performing global searches of trajectories. The advantages of this procedure will be clearer in the following sections.

IV.VI Keplerian map update

These estimates of the perturbed motion can be used to update the orbital elements of an object at each periapsis passage.

Given a set of Keplerian elements of an object at its periapsis at an epoch, the angular distance α can be readily computed as:

$$\alpha_0 = \Omega_{rot} + \arctan(\cos i_0 \cdot \tan \omega_0) \quad (23)$$

where Ω_{rot} is $\Omega_0 - \nu_{\oplus}$, ν_{\oplus} is the true anomaly of the Earth and the subscript 0 indicates the set of orbital elements before the first update.

Knowing α_0 , the update on $(a_0, e_0, i_0, \omega_0)$ is defined by Eq.(15), (17), (18) and (22). At the next periapsis passage, α_0 is updated by the mutual drift between the object and the Earth, as well as by the changes in Ω due to perturbations in inclination and argument of the periapsis:

$$\alpha_{n+1} = \alpha_n + 2\pi \left| \sqrt{\frac{a_{n+1}^3}{(1-\mu)} - 1} \right| \quad (24)$$

$$+ \text{atan}(\cos i_{n+1} \cdot \tan \omega_{n+1}) - \text{atan}(\cos i_n \cdot \tan \omega_n)$$

where subscript n represent the iteration number.

V. ENCOUNTER MAP

The Keplerian map, introduced in the previous section, fails however in two important aspects when used to provide a good understanding of how the next planetary encounter will change the orbital elements of an asteroid. Firstly, if we define as an Earth encounter the period of time that an asteroid is close enough to Earth that its gravitational effect is non-negligible, the Keplerian map fails to provide a complete picture of what occurs during an encounter, since an asteroid may undergo several periapsis passages during this time. It often happens that if an asteroid suffers several *kicks* these may partially cancel each other out.

The second drawback is that it is difficult to know which is the angular α region of interest, since some orbits will *feel* the Earth at longer angular distances. The latter is of course not due to a magical increase in the gravity of the Earth, but a consequence of using the periapsis passage as a representation of the effect of the Earth on the entire orbit of the asteroid.

Hence, it is hereafter referred as *encounter map* the added effect of all periapsis passages that an asteroid undergoes during the time the asteroid remains within a $\pi/8$ angular distance from the Earth-Sun line. As discussed in [3], this angular distance corresponds roughly to a distance from Earth of the order of 0.4 AU, where the gravitational influence of the planet is considered small.

As an example, we can now reproduce the semi-major axis and inclination encounter map for asteroid 2012 LA. Figure 10 and Figure 11 evidence the difference between the Keplerian map and the encounter map. In a sense, the encounter map is the summary of the integrated Earth's disturbance during the period of time the asteroid is within 0.4 AU distance from the Earth. Figure 10 and Figure 11 also show the numerical results of the Earth's perturbation and the predicted effect of the encounter that 2012 LA will undergo in 2029. In this occasion, the numerical validation using the CR3BP is done by propagating the different initial conditions at the $+\pi/8$ until these cross the section $-\pi/8$. Finally, these figures evidence the use of angle α as a target parameter that uniquely defines an encounter and the effects of it.

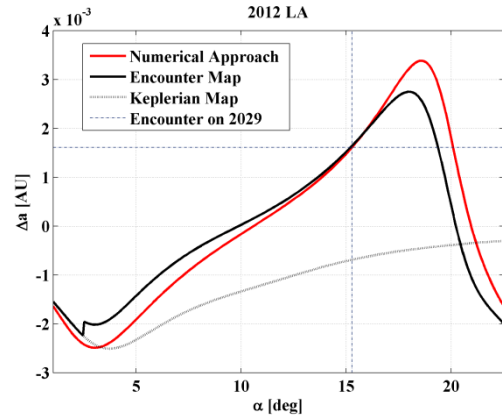


Figure 10: Semi-major axis *encounter map* as a function of the angular distance of the periapsis passage for a 2012 LA-like orbit (1.04 AU, 0.023, 3.13 deg).

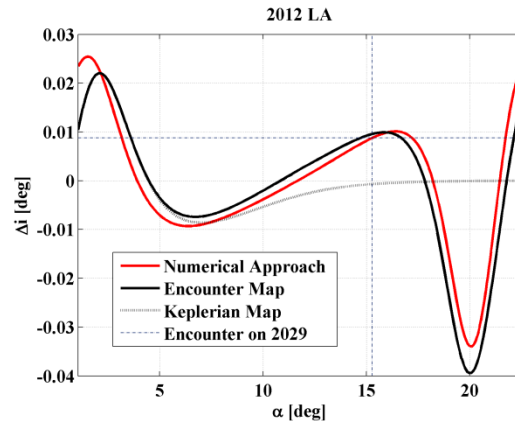


Figure 11: Inclination *encounter map* as a function of the angular distance of the periapsis passage for a 2012 LA-like orbit (1.04 AU, 0.023, 3.13 deg).

V.I Search for resonant encounters

The tool described above can now be used to perform a rapid search for advantageous resonant encounters with the Earth that may decrease the estimated cost of an asteroid capture transfer. As

discussed previously, hauling a large asteroid back to Earth with today's propulsion technology requires extremely low energy trajectories. Thus, albeit much longer times of flight are expected, sequences of Earth encounters may ease enormously the technology necessary to carry out this type of missions.

As described in [3], asteroid 2009 BD could potentially be inserted into a vertical Lyapunov orbit near the L_2 point with a 490 m/s transfer starting on 28th February 2021 and finishing on 21st September 2025, thus a 4.5 years long transfer. However, if unperturbed this asteroid will undergo an encounter with the Earth early on 2023. The encounter is depicted in Figure 12, together with the capture alternative during the first Earth encounter.

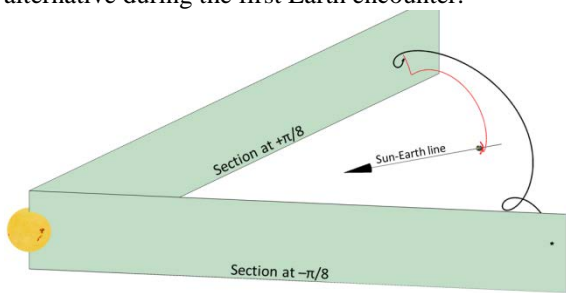


Figure 12. Schematic of the current (i.e., unperturbed) encounter geometry (black trajectory) and example of capture trajectory (red trajectory).

Despite the fact that the unperturbed 2009 BD will enter the region within a $\pi/8$ angular distance from the Sun-Earth line, the asteroid will remain relatively far from the Earth while crossing this region, and thus, it is expected that the Earth's disturbance will be small. This is more clearly shown in the encounter maps for semi-major axis, eccentricity and argument of the periapsis shown in Figure 13, 14 and 15 respectively, where a vertical and horizontal dotted line have been added to represent the unperturbed target α angle and the consequences of that approach.

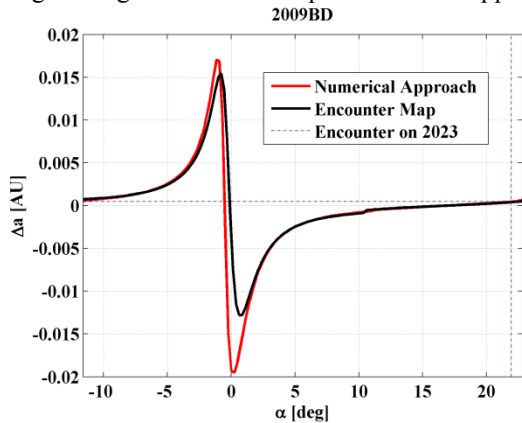


Figure 13. Semi-major axis encounter map as a function of the angular distance α for 2009 BD (1.06 AU, 0.05, 1.26 deg).

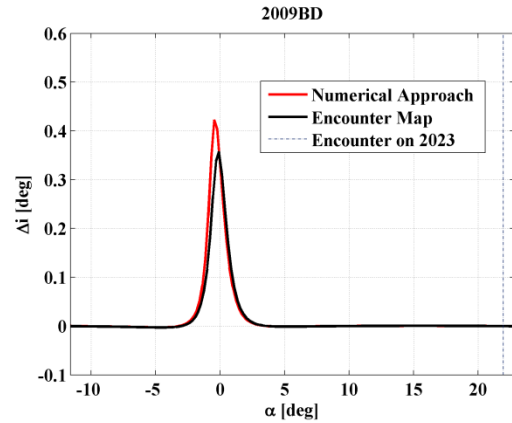


Figure 14. Inclination encounter map as a function of the angular distance α for 2009 BD (1.06 AU, 0.05, 1.26 deg).

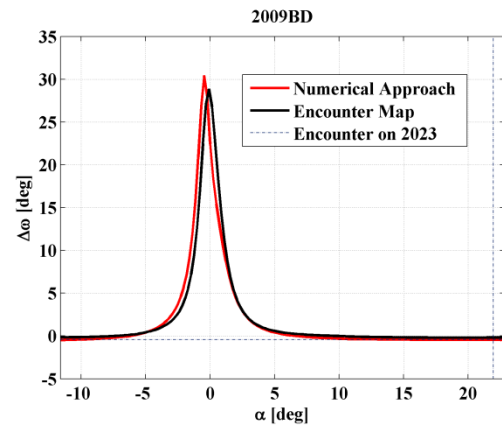


Figure 15. Argument of the periapsis ω encounter map as a function of the angular distance α for 2009 BD (1.06 AU, 0.05, 1.26 deg).

Once the encounter map of an asteroid is computed, the filter described in Section IV.I can be used to rapidly assess the convenience of a resonant encounter with the Earth. Figure 16 summarizes the Δv gain for an Earth-Earth sequence, as opposed to the direct capture of asteroid 2009 BD during the first Earth encounter, whose optimized solution required 490 m/s [3].

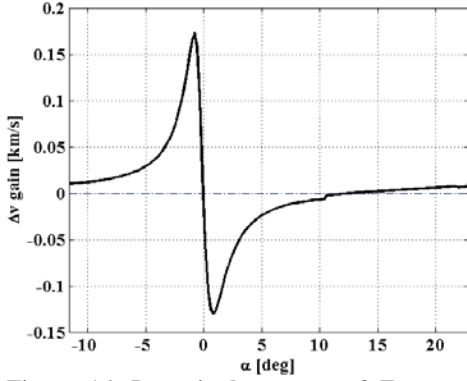


Figure 16. Dv gain by means of Encounter Map prediction.

In order to compute Figure 16, an impulsive manoeuvre is assumed at the periaapsis closest to the section $-\pi/8$, but outside the encounter region. Bear in mind that asteroids with semi-major axis larger than 1 AU will, in average, move clockwise relatively to the Earth.

This periaapsis burn is intended to adjust the period of the asteroid in order to modify the angle α as required for the following encounter. Hence, if we require a shift the encounter angle by a $\Delta\alpha$, the required change in semimajor axis Δa is estimated as:

$$\Delta a = \frac{\sqrt{1-\mu} \cdot \Delta\alpha}{3\pi n_p \sqrt{a}} \quad (25)$$

where n_p is the number of complete orbits from the manoeuvre to the first periaapsis passage within the encounter region.

The cost of the manoeuvre to provide a change in semi-major axis as in Eq. (25) can be estimated using the Gauss' form of the variational equations:

$$\Delta v_\alpha = \frac{\mu_\odot \Delta a}{2a^2 v_p} \quad (26)$$

where μ_\odot is the Sun's gravitational constant and v_p the velocity at the periaapsis and Δv_α is assumed in the tangential direction. Note that as a consequence of this phasing manoeuvre, the eccentricity is also changed by:

$$\Delta e = \frac{2(e+1)}{v_p} \Delta v_\alpha \quad (27)$$

Hence, given a targeted encounter (i.e., defined by α), the Keplerian elements of the asteroid can be updated by means of Eq. (25), (27) and the encounter map previously computed. After that, the filter described in Section IV.I is used to come up with the

lowest Δv estimate to target one of the 500 hyperbolic invariant manifold trajectories stored for the same Jacobi constant and type of LPO as the trajectory we want to improve, as computed in [3]. The result is then compared, not with the optimized trajectory, but also with the filter estimate for a capture to the same Jacobi constant and type of LPO as on the optimized trajectory. The latter is done to ensure a fair comparison.

VI. EARTH RESONANT CAPTURE

In this final section, the most promising asteroids found in [3] are reviewed in search of opportunities for quasi-ballistic capture by means of multiple resonant encounters with the Earth.

The list of promising asteroid targets for retrieval was built by 24 different objects whose filter estimate for capture in one of the LPO stable manifold sets was lower than 1 km/s. This list was built by 7 Amor asteroids, 12 Apollo and 5 Atens. Since the Keplerian map approach assumes that the encounter occurs outside the sphere of influence of the Earth, only Amor objects could be considered now for analysis. Alternatives to circumvent this issue and extend the utilization of this tool to other types of orbits are discussed though in Section VII, which is left for future work.

Table 2 shows the results of the search for sequences of beneficial resonant encounter with the Earth. This search was carried out by a global optimization carried out with Matlab's *ga* function (genetic algorithm). The search was aimed to find the optimal sequence of α angles that allowed for an optimal change in Keplerian elements, and thus minimizing the final capture manoeuvre for insertion into the stable manifold trajectory that delivers the asteroid into a periodic bound orbit. The sequences of Earth encounter were estimated by means of the encounter map calculated with the orbital elements of the asteroid previous to the first encounter.

Two asteroids seem to be particularly suited to benefit from multiple Earth encounters, 2011 MD and 2009 BD. These two objects achieves important reductions of the nominal Δv costs, for capture at the first encounter, around 7 and 3 -fold reductions respectively are achieved. On the other hand, other asteroids seem to be particularly immune to further three body-benefits. All of these trajectories require the increase of the transfer time of flight by several decades, which is a direct consequence of the synodic period, thus the time between consecutive encounters.

		Capture at First Encounter				Resonant Capture (Optimal Δv Gain/ToF)			Resonant Capture (Maximum Δv reduction)		
		Target LPO	Optimal Traj. [m/s]	Filter Estimate [m/s]	ToF [Years]	Sequence	Δv Gain [m/s]	ToF [Years]	Sequence	Δv Gain [m/s]	ToF [Years]
1.	2011BL45	2V	400	387	6,3	EE	-38	27,5	EEEE	-68	97,4
2.	2012LA	2V	544	436	4,4	EE	-26	23,0	EEEE	-54	82,3
3.	2011MD	2V	422	421	4,3	EE	-95	19,2	EEEE	-359	81,7
4.	2011MD	2Hs	986	886	4,4	EEE	-46	35,9	EEEE	-47	70,8
5.	2011MD	2Hn	976	905	5,5	EEE	-23	32,1	EEEE	-32	45,0
6.	2009BD	2V	493	468	4,6	EE	-130	19,8	EEEE	-295	59,8
7.	2009BD	2P	687	608	2,5	EE	0	14,0	EE	0	14,0
8.	2009BD	2Hs	399	411	4,6	EE	-45	18,9	EEE	-54	32,2
9.	2009BD	2Hn	714	641	4	EE	-33	17,4	EEEE	-44	52,4
10.	2008HU4	2V	772	758	3,2	EE	-79	12,0	EEE	-138	21,9
11.	2008HU4	2P	728	717	5,8	EEE	-83	24,3	EEEE	-90	41,3
12.	2008HU4	2Hs	663	575	4,7	EE	-58	13,4	EEEE	-107	34,0
13.	2008HU4	2Hn	892	644	2,9	EE	-39	11,7	EEE	-60	21,5
14.	1993HD	2P	712	689	4,2	EEE	0	17,0	EEE	0	17,0
15.	1993HD	2Hs	881	836	1,7	EE	-8	9,5	EEEE	-15	32,5
16.	1993HD	2Hn	851	835	3,5	EE	-8	11,4	EEEE	-11	24,4

Table 2: Capture trajectories and mass estimates for the best trajectory of each type.

VII. CONCLUSIONS AND FUTURE WORK

The work presented in this paper consists of two distinct parts: The first one is the on-going work on the asteroid retrieval problem, the second part is the development of a tool to describe semi-analytically the motion of a test particle (i.e., spacecraft or asteroid) in the CR3BP. These two parts will be discussed separately in this final section.

VII.I Keplerian and encounter map approximation

This paper has discussed the early development of a semi-analytical general perturbation method to describe the motion of an object in the CR3BP. This method is based on a description of the CR3BP Hamiltonian with a series expansion in μ retaining only the first order perturbation.

The tool has been validated by constantly comparing the Keplerian and encounter map estimates with the equivalent motion propagated with the CR3BP. By doing so, it can be concluded that the estimates given by the Keplerian map are accurate for types of orbits that remain relatively clear of the sphere of influence of the Earth and, thus, can be used for preliminary trajectory design in those cases. The fact that the tool uses classical orbital elements is also of some advantage for that purpose.

The tool has been applied here to Amor type of asteroids, which remain relatively far from the sphere of influence of the Earth. However, it can also be successfully applied to other types of orbits, systems (e.g., Earth-Moon, Jupiter-Moons) and mission requirements (e.g., End-of-life, or disposal trajectories) [8]. The out-of-plane extension proposed here, with respect previous developments [4], has represented a significant advantage, since small variation of inclination yield large Δv gains.

However, the integrations are currently implemented as numerical quadratures and no substantial time gain is achieved by using this tool. Nevertheless, future work should speed up the process by analytically solving the integrations, or parts of them, and thus gaining some competitive advantage over the option of performing a numerical propagation in the CR3BP.

VII.II Easily Retrievable Objects

The paper has explored the possibility of using multiple resonant encounters with the Earth on a reduced group of six asteroids (corresponding to Amors). The best retrieval options for capture at the first encounter required more than 400 m/s in order to place these objects in trajectories that lead to bound motion near the Earth. By carrying out a search using the algorithms developed in this paper several combinations of Earth encounters have been found that substantially reduce the capture requirements (see Table 2).

Clearly, the drawback of these trajectories is that the time required to fly them is on the order of a few decades. However, in some instances, these trajectories may be necessary to allow space technology the capability to haul large masses. For example, asteroids 2009 BD and 2011 MD would not be able to be captured at the first Earth encounter due to the large Δv requirement, their expected mass ($>10^6$ kg) and current propulsion technology [9], while at the current propulsion capability these objects could be captured with the encounter sequences found here. Lastly, it is also of interest to note that some asteroids seem to obtain little advantage from multiple Earth encounters, such as the case of 1993 HD.

ACKNOWLEDGEMENTS

The work reported was supported by European Research Council grant 227571 (VISIONSPACE) and the Marie Curie grant 330649 (AsteroidRetrieval).

APPENDIX

Semi-major axis kick

$$\Delta a = \frac{2\mu}{an^2} \int_{-\pi}^{\pi} \frac{\partial R}{\partial v} dv$$

$$\frac{\partial R}{\partial v} = \frac{1}{(1+r^2-2r\cos\theta)^{3/2}} \left(r^2 \left(\frac{e\sin v}{1+e\cos v} \right) - \left(r \left(\frac{e\sin v}{1+e\cos v} \right) \cos\theta - r \frac{\partial \cos\theta}{\partial v} \right) \right)$$

$$+ \left(\frac{1}{p^2} \right) \left[(1+e\cos v)^2 \frac{\partial \cos\theta}{\partial v} - 2(1+e\cos v)e\sin v \cos\theta \right] - \frac{e\sin v}{p}$$

$$\frac{\partial \cos\theta}{\partial v} = -[\cos\Omega_{rot} \cdot \sin(v+\omega) + \sin\Omega_{rot} \cdot \cos(v+\omega) \cdot \cos i]$$

Inclination kick

$$\Delta i = \frac{\mu}{n^2 a^4 b^2 \sin i} \left(\cos i \int_{-\pi}^{\pi} r^2 \frac{\partial R}{\partial \omega} dv - \int_{-\pi}^{\pi} r^2 \frac{\partial R}{\partial \Omega} dv \right)$$

$$\frac{\partial R}{\partial \Omega} = \frac{r(\sin\Omega_{rot} \cos(v+\omega) + \cos\Omega_{rot} \cdot \sin(v+\omega) \cdot \cos i)}{(1+r^2-2r\cos\theta)^{3/2}} - \frac{\sin\Omega_{rot} \cdot \cos(v+\omega) + \cos\Omega_{rot} \cdot \sin(v+\omega) \cdot \cos i}{r^2}$$

$$\frac{\partial R}{\partial \omega} = \frac{r(\cos\Omega_{rot} \cdot \sin(v+\omega) + \sin\Omega_{rot} \cdot \cos(v+\omega) \cdot \cos i)}{(1+r^2-2r\cos\theta)^{3/2}} - \frac{\cos\Omega_{rot} \cdot \sin(v+\omega) + \sin\Omega_{rot} \cdot \cos(v+\omega) \cdot \cos i}{r^2}$$

Argument of periapsis kick

$$\Delta \omega = \frac{1}{n^2 a^4 e} \int_{-\pi}^{\pi} r^2 \frac{\partial R}{\partial e} dv - \frac{\cos i}{(nab)^2 \sin i} \int_{-\pi}^{\pi} r^2 \frac{\partial R}{\partial i} dv$$

$$\frac{\partial R}{\partial e} = -\frac{1}{r^2} \frac{dr}{de} - 2 \frac{\cos\theta}{r^3} \frac{dr}{de} + \frac{(r-\cos\theta)}{(1+r^2-2r\cos\theta)^{3/2}} \frac{dr}{de}$$

$$\frac{dr}{de} = -\frac{-2ea}{1+e\cos v} - \frac{a(1-e^2)\cos v}{(1+e\cos v)^2}$$

$$\frac{\partial R}{\partial i} = \left(\frac{1}{r^2} - \frac{r}{(1+r^2-2r\cos\theta)^{3/2}} \right) \sin\Omega_{rot} \sin(\omega+v) \sin i$$

REFERENCES

- | | |
|--|--|
| <p>[1] Elvis, M., "Let's Mine Asteroids — for Science and Profit," <i>Nature</i>, Vol. 485, No. 7400, 2012, p. 549. doi: 10.1038/485549a</p> <p>[2] Brophy, J. and et.al, "Asteroid Retrieval Feasibility Study," Keck Institute for Space Studies, California Institute of Technology, Jet Propulsion Laboratory, 2012.</p> | <p>[3] García Yáñez, D., Sanchez, J. P. and McInnes, C. R., "Easily Retrievable Objects among the Neo Population," <i>Celestial Mechanics and Dynamical Astronomy</i>, 2013, pp. 1-22. doi: 10.1007/s10569-013-9495-6</p> <p>[4] Ross, S. D. and Scheeres, D. J., "Multiple Gravity Assists, Capture, and Escape in the Restricted Three-Body Problem," <i>SIAM J. Applied Dynamical Systems</i>, Vol. 6, No. 3, 2007, pp. 576-596. doi: 10.1137/060663374</p> |
|--|--|

- [5] Hollenbeck, G. R., "New Flight Techniques for Outer Planet Missions," *Astrodynamics Specialist Conference, Nassau, Bahamas, July 28-30, 1975, AAS 26 p.*, American Astronautical Society and American Institute of Aeronautics and Astronautics, 1975.
- [6] Johannesen, J. and D'Amario, L., "Europa Orbiter Mission Trajectory Design," *Astrodynamics Specialist Conference, AAS/AIAA, Girdwood, Alaska, USA, 1999.*
- [7] Vallado, D. A., *Fundamentals of Astrodynamics and Applications*, Third Edition, The Space Technology Library, Microcosm Press and Springer, Hawthorne Press, 2007.
- [8] Alessi, E. M., Colombo, C., Sanchez Cuartielles, J. P. and Landgraf, M., "Out-of-Plane Extension of Resonant Encounters for Escape and Capture," *Proceedings of the 64rd International Astronautical Congress, IAF, China, Beijing, 2013.*
- [9] Brophy, J., "The Dawn Ion Propulsion System," *Space Science Reviews*, Vol. 163, No. 1, 2011, pp. 251-261. doi: 10.1007/s11214-011-9848-y